



Defect-induced room temperature ferromagnetism in Fe and Na co-doped ZnO nanoparticles

Hao Gu^a, Yinzhu Jiang^{b,*}, Mi Yan^{a,*}

^a State Key Laboratory of Silicon Materials, Department of Materials Science and Engineering, Zhejiang University, Hangzhou 310027, China

^b Department of Materials Science and Engineering, Zhejiang University, Hangzhou 310027, China

ARTICLE INFO

Article history:

Received 17 August 2011

Received in revised form 6 January 2012

Accepted 9 January 2012

Available online 15 January 2012

Keywords:

Semiconductors

Sol-gel

Magnetic properties

ZnO

ABSTRACT

The effect of defects in the diluted magnetic semiconductor (DMS) of Fe and Na co-doped ZnO nanoparticles was investigated. Structural characterizations revealed that Fe and Na ions enter into ZnO lattice without any secondary phase. The ferromagnetic behaviors at room temperature were found in all samples, which are attributed to the exchange via electron trapped oxygen vacancies (F-center) coupled with magnetic Fe ions. With the increase of the Na concentration, the oxygen vacancy mediated ferromagnetic state is enhanced. The observed correlation between the Na concentration, the carrier concentration and the magnetization revealed the role of the defect in tuning the ferromagnetism in the ZnO-based DMS system.

© 2012 Published by Elsevier B.V.

1. Introduction

In the field of spintronics, diluted magnetic semiconductors (DMSs) are getting more and more attention for their potential applications in information storage and microelectronics industry [1–5]. Since oxide semiconductor based DMSs doped by 3d transition metal (TM) elements (Co, Fe, Mn, V, etc.) were proved to show ferromagnetism above room temperature both in theory [6,7] and experiment [8–12]. A lot of further researches concerning their ferromagnetism mechanisms and the impact factors have been carried out, and various debates are never scarce. In recent research works, additional defects such as oxygen vacancies or H interstitials were proved to play an important role in establishing or enhancing the magnetic couplings both in oxides compound [13–15] and doping compounds [16–18]. Many types of oxide semiconductors such as HfO₂, CeO₂, CaO, etc. [19] are found to be ferromagnetic, and it is attributed to the existence of vacancies and interstitials for there is no magnetic ions were introduced. While in TM doped oxide semiconductors, it is possible to control the magnetizations by changing the concentration of doping ions which leads to the variation of defects, so it has attracted a lot of interests. Sato and Katayama-Yoshida [20] used first principles calculations to predict that hole doping in Fe-doped ZnO DMS will weaken the primarily internal ferromagnetism, but Gopal and Spaldin [7] held the conclusion that p-type Li co-dopants might result in room temperature ferromagnetism in Fe-doped ZnO through ab initio calculations. Schwartz

and Gamelin [21] demonstrated experimentally that by introducing and removing interstitial Zn(Zn_i), a native n-type defect of ZnO, the magnetic coupling could be changed in ZnO based DMS. Also, Jayakumar et al. [22] showed this experimentally by introducing H as a shallow donor in Li and Co co-doped ZnO to tune the sample from paramagnetic to ferromagnetic state. But actually, there is also no direct evidence given to demonstrate the way how defects give raise to ferromagnetism. Since Na ions in ZnO is a promising candidate of p-type dopant and without its own 3d electrons to interfere with magnetic ordering, it offers an opportunity to explore the role of defect in influencing the magnetic orderings. In this work, Na was introduced into Fe-doped ZnO DMS by sol-gel method, in order to get insight into the role of defects and their influence to the magnetic properties. We chose 5% Fe doping in ZnFeNaO samples for the reason that room temperature ferromagnetism in 5% Fe doped ZnO is now well established according to our previous work and the magnetization of 5% Fe doped ZnO can be considered comprehensively as an optimum value. Strong room temperature ferromagnetism relying on the Na concentration was observed, showing clearly the effect of defects in making the magnetic interactions between Fe ions more efficient.

2. Experimental

A group of polycrystalline Zn_{0.95-x}Fe_{0.05}Na_xO (x = 0, 0.01, 0.05 and 0.10) nanoparticles were synthesized by sol-gel method. Weighed quantities of zinc acetate (Zn(CH₃COO)₂), ferrous acetate (Fe(CH₃COO)₂) and sodium acetate (CH₃COONa) powders were first mixed and then dissolved in the solution of ethylene glycol monomethyl ether (C₃H₈O₂), adding a small amount of ethanolamine (C₂H₇NO) during the liquid stirring until when a pellucid red solution was obtained. All these procedures were carried out in the air at room temperature. After a 36 h sol aging

* Corresponding authors. Tel.: +86 571 8795 2366.

E-mail addresses: yzjiang@zju.edu.cn (Y. Jiang), mse.yanmi@zju.edu.cn (M. Yan).

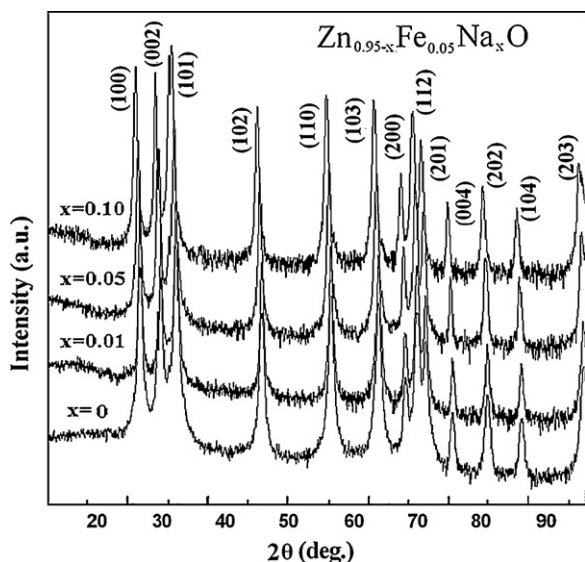


Fig. 1. XRD patterns of $\text{Zn}_{0.95-x}\text{Fe}_{0.05}\text{Na}_x\text{O}$ ($x=0, 0.01, 0.05, 0.10$) samples at room temperature.

stage, the solution was dried for 48 h at 90 °C to form gel in vacuum ($\sim 10^{-2}$ Pa). The dried gel was annealed for 3 h at 300 °C in vacuum ($\sim 10^{-2}$ Pa).

The crystal structures of these samples were characterized by a Rigaku D/max 2550PC X-ray diffractometer with $\text{Cu K}\alpha$ radiation. High-resolution transmission electron microscopy (HRTEM) imaging and selected area electron diffraction (SAED) studies were carried out with a JEOL JEM 2010 transmission electron microscopy (TEM). X-ray photoelectron spectroscopy (XPS) was employed by using a PerkinElmer PHI-5000C ESCA system with $\text{Al K}\alpha$ radiation. All binding energies were calibrated by using the containment carbon ($\text{C}_{1s} = 284.8$ eV) as a reference. Carrier densities of samples were studied by Bio-Rad microscience HL5500 Hall system. Magnetization measurements for $\text{Zn}_{0.95-x}\text{Fe}_{0.05}\text{Na}_x\text{O}$ nanoparticles were carried out by a Lakeshore 7407 vibrating sample magnetometer (VSM).

3. Results and discussion

Fig. 1 presents the XRD patterns for $\text{Zn}_{0.95-x}\text{Fe}_{0.05}\text{Na}_x\text{O}$ ($x=0, 0.01, 0.05, 0.10$) nanoparticles in log-scale. As can be seen, the doping of Fe and Na does not disturb the wurtzite structure of ZnO, even when the concentration achieves 10% level, surpassing 7% as the highest doping level by sol-gel method [23] or 8% as the theoretical doping limit [24] reported. $\text{Zn}_{0.95-x}\text{Fe}_{0.05}\text{Na}_x\text{O}$ ($x=0, 0.01, 0.05, 0.10$) samples at room temperature was detected to be wurtzite structure with space group of $P63mc$. The lattice parameters and unit cell volumes of all the samples are shown in **Table 1**. The

Table 1

Lattice parameters and unit cell volumes of $\text{Zn}_{0.95-x}\text{Fe}_{0.05}\text{Na}_x\text{O}$ ($x=0, 0.01, 0.05, 0.10$) powder samples at room temperature, which were obtained from X-ray diffraction patterns.

x	a_0 (Å)	c_0 (Å)	Cell V (Å ³)
0	3.2554	5.2135	47.85
0.01	3.2588	5.2187	47.97
0.05	3.2675	5.2343	48.30
0.10	3.2754	5.2553	48.63

increased lattice parameter values with increment of Na concentration is attributed to the larger ion radius of Na^+ (0.97 Å) compared with that of Fe^{2+} (0.74 Å) and Zn^{2+} (0.74 Å). Moreover, no other phases like magnetite (Fe_3O_4), Fe clusters or ZnFe_2O_4 was showed in these XRD patterns, and it may be attributed to the limitation of XRD characterization that small amount of impurities cannot be detected.

Sample of $\text{Zn}_{0.85}\text{Fe}_{0.05}\text{Na}_{0.1}\text{O}$ which contains the maximum content of Na was characterized by TEM, HRTEM and SAED analysis. It can be seen that the sample was highly agglomerated as polycrystalline particles with the size in range of 30–80 nm as shown in **Fig. 2(a)**. The HRTEM images of these particles shown in **Fig. 2(b)** show a defect free structure and no detectable trace of impurities present in the sample. The SAED pattern from a finely dispersed region as depicted in the inset of **Fig. 2(b)** shows that the rings made up of discrete spots indicating the highly crystalline nature of nano particulates, which is also consistent with the wurtzite ZnO structure with intense ring pattern in the electron diffraction pattern.

The valence of Fe in $\text{Zn}_{0.95-x}\text{Fe}_{0.05}\text{Na}_x\text{O}$ ($x=0, 0.01, 0.05, 0.10$) samples was characterized by the core-level XPS spectrum measurements, and the results of $\text{Zn}_{0.85}\text{Fe}_{0.05}\text{Na}_{0.1}\text{O}$ samples are shown in **Fig. 3**. Wide-scan XPS scan is shown in **Fig. 3(a)**, and no magnetic contamination or pre-cursor element was found. It can be seen from **Fig. 3(b)** that the Fe $2p_{1/2}$ and $2p_{3/2}$ peaks are located at 722.7 eV and 709.4 eV, respectively. The position of these primary peaks is consistent with that of the core-level XPS spectrum of Fe^{2+} ions in FeO single crystal (722.3 eV for Fe $2p_{1/2}$ and 709.3 eV for Fe $2p_{3/2}$) as found in the previous experiment [25]. No Fe^{3+} in Fe_2O_3 (724.9 eV for Fe $2p_{1/2}$ and 710.7 eV for Fe $2p_{3/2}$) or metallic Fe^0 (719.9 eV for Fe $2p_{1/2}$ and 706.7 eV for Fe $2p_{3/2}$) was observed in the spectra [26]. Similar results have been detected in other $\text{Zn}_{0.95-x}\text{Fe}_{0.05}\text{Na}_x\text{O}$ ($x=0, 0.01, 0.05$) samples. Based on the XPS results, Fe chemical states in $\text{Zn}_{0.95-x}\text{Fe}_{0.05}\text{Na}_x\text{O}$ samples are believed to be Fe^{2+} as substitution state, similar to the reports on the ZnFeO system by

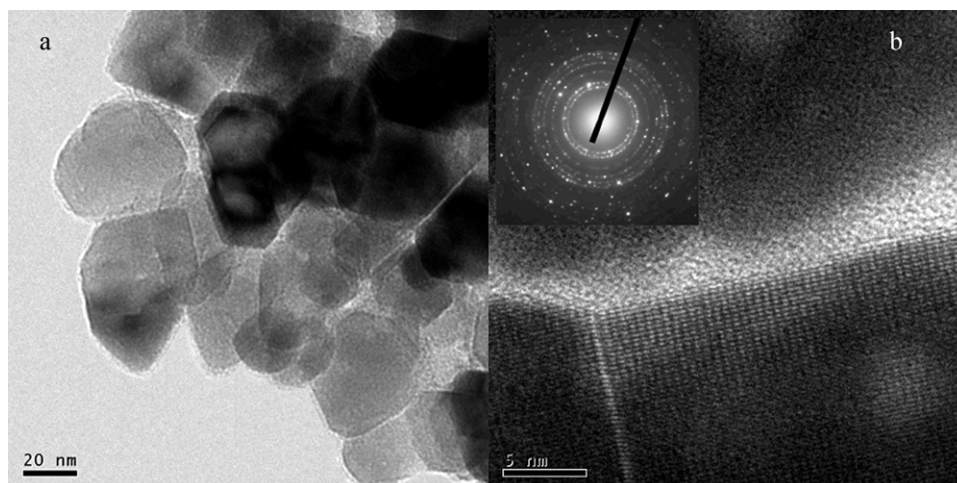


Fig. 2. (a) TEM, (b) HRTEM and SAED analysis of $\text{Zn}_{0.85}\text{Fe}_{0.05}\text{Na}_{0.1}\text{O}$ nanoparticles.

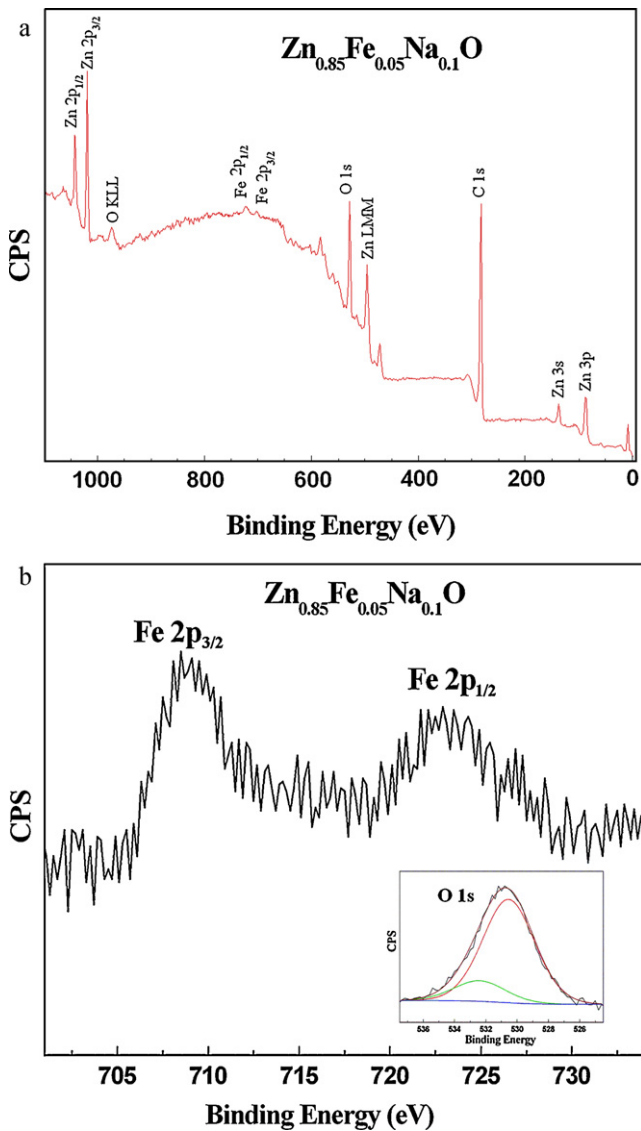


Fig. 3. (a) The wide scan XPS spectra and (b) core-level XPS spectrum of Fe 2p and O 1s (inset) for $\text{Zn}_{0.85}\text{Fe}_{0.05}\text{Na}_{0.1}\text{O}$ sample.

other studies [27,28], which reveals that the chemical state of Fe in Fe doped ZnO changes from Fe^{3+} to Fe^{2+} with an increase in the amount of Fe dopant and Fe chemical states in $\text{Zn}_{1-x}\text{Fe}_x\text{O}$ ($x \geq 2.6$ at.%) are found to be Fe^{2+} .

Fig. 4(a) shows the magnetization hysteresis loops at room temperature for $\text{Zn}_{0.95-x}\text{Fe}_{0.05}\text{Na}_x\text{O}$ ($x=0, 0.01, 0.05, 0.10$), and the inset of Fig. 4(a) depicts the measurements with a smaller maximum magnetic field for the samples of $\text{Zn}_{0.95-x}\text{Fe}_{0.05}\text{Na}_x\text{O}$. From these loops, remarkable ferromagnetic behaviors can be observed in all of the samples with the coercivity (H_c) ranging from 24 to 60 Oe. Magnetizations in all the samples get nearly saturated at ~ 1.2 kOe. The values of M_s , M_r and H_c for all $\text{Zn}_{0.95-x}\text{Fe}_{0.05}\text{Na}_x\text{O}$ samples are listed in Table 2. The saturation magnetization (M_s) enhances with the Na concentration grows, and it reaches its peak value as 0.32 emu/g, much larger than 0.09 emu/g, the M_s value of sample $\text{Zn}_{0.95}\text{Fe}_{0.05}\text{O}$, also much larger than most of the values for $\text{Zn}_{0.95}\text{Fe}_{0.05}\text{O}$ as recently reported [23,29]. This result should be ascribed to the variation of related defects caused by Na co-doping, and is in quite difference from the calculation results of Sato and Katayama-Yoshida [20] in their theoretical pattern, when the Fe doping level is under 10%, hole doping will cause a slight advantage for spin-glass state over ferromagnetic state and this weak

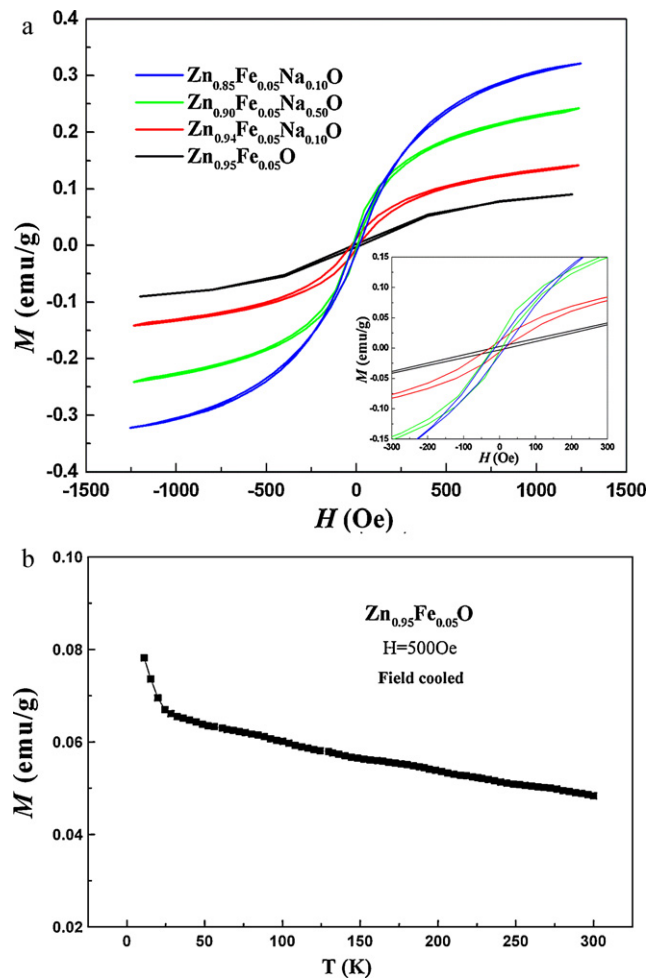


Fig. 4. (a) The temperature dependent magnetization for $\text{Zn}_{0.95}\text{Fe}_{0.05}\text{O}$ sample, (b) M - H loops of $\text{Zn}_{0.95-x}\text{Fe}_{0.05}\text{Na}_x\text{O}$ ($x=0, 0.01, 0.05, 0.10$) nanoparticles at room temperature. The inset depicts the measurements with a smaller maximum magnetic field for the samples of $\text{Zn}_{0.95-x}\text{Fe}_{0.05}\text{Na}_x\text{O}$.

ascendancy will almost be invariant when the hole concentration exceeds 15%. However, our experimental results exhibit ferromagnetism at room temperature. The temperature dependence of magnetization of $\text{Zn}_{0.95}\text{Fe}_{0.05}\text{O}$ under an applied field of 500 Oe is also presented in Fig. 4(b). The magnetization was increased with decrease of temperature, also indicating the S shaped curves arise from ferromagnetism by $\text{Zn}_{0.95}\text{Fe}_{0.05}\text{O}$. At the same time, room temperature ferromagnetism was observed and no transition to ferromagnetism occurs in lower temperature. This is consistent with the results of Raley et al. [30] and Jayakumar et al. [31].

The room temperature ferromagnetism for the samples of Na and Fe co-doped ZnO can be attributed to Fe and Na ions rather than any precipitates such as TM clusters or TM oxides which have been ruled out through the XRD and XPS measurements. Further more, the magnetic orderings would not change significantly with the increase of Na concentration if the ferromagnetism is attributed

Table 2

The values of M_s , M_r and H_c for all $\text{Zn}_{0.95-x}\text{Fe}_{0.05}\text{Na}_x\text{O}$ ($x=0, 0.01, 0.05, 0.10$) samples are listed in a table as follows, and added to the revised manuscript.

x	M_s (emu/g)	M_r (emu/g)	H_c (Oe)
0	0.09	0.00285	60
0.01	0.14	0.00946	48
0.05	0.24	0.01124	24
0.10	0.32	0.01325	30

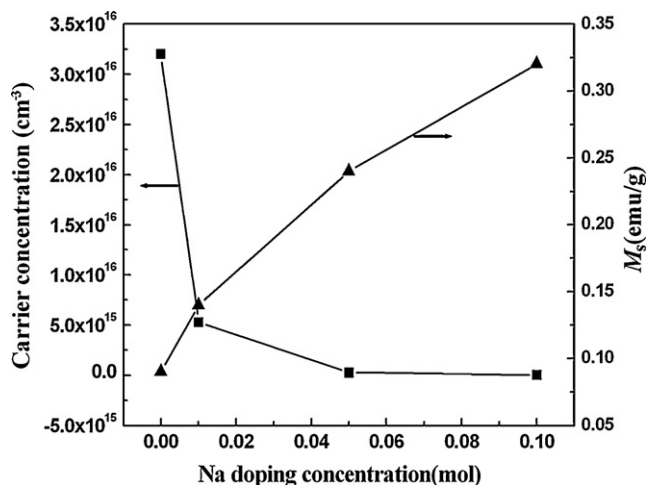


Fig. 5. Carrier concentration and variations of saturation magnetization (M_s) of $Zn_{0.95-x}Fe_{0.05}Na_xO$ ($x=0, 0.01, 0.05, 0.10$) nanoparticles at 300 K.

to Fe clusters or Fe oxides. In our previous work [32], the magnetic measurements for the ZnNaO samples show nearly straight lines indicating diamagnetism, which manifests the impossibility of introducing magnetism by Na^+ alone. The overlapping loops of the $Zn_{1-y}Na_yO$ ($y=0.01, 0.05, 0.10$) confirm that the magnitude of Na^+ has no influence on the magnetization in the ZnNaO structure. Considering the fact that the radii of Zn^{2+} (0.74 Å) similar to that of Fe^{2+} (0.72 Å), it is rational to speculate that the lattice sites occupied by Na^+ (0.97 Å) ions keep identical in the ZnFeNaO to that in the ZnNaO samples. It is noted that ZnO is a native n-type semiconductor for the presence of interstitial Zn and hydrogen contamination during its growth, and some researchers indicated that Na ions enter into ZnO lattice and form relative defects such as hole doping or electron doping [33–35]. It has been shown that the interstitial Li/Na is more stable than substitutional ones by local density functional calculations [36]. Also Lee and Chang [33] reported that substitutional Li and Na are better acceptors in ZnO with shallow acceptor level by using first-principles density functional calculations. The XPS scan of Na 1s peak presented a +1 ionization state, and we also got the O1s XPS spectra of $Zn_{0.85}Fe_{0.05}Na_{0.1}O$ sample in the inset of Fig. 3(b), and position of O 1s peaks is found to be 531.4 eV, which is the contributions from oxygen of ZnO (530.8 eV) and partially from Na–O–Na bonding (531.75 eV) [37]. This indicates that the Na ions enter into ZnO lattice and substitute Zn atoms to form Na–O–Na bonds [38], and the oxygen vacancies arise naturally to ensure charge neutrality when a univalent Na ion substitutes Zn ion in ZnO.

Carrier densities of all the samples were characterized by Hall-effect measurement as shown in Fig. 5. It can be seen that Fe and Na co-doping ZnO samples are all n-type semiconductors, and the carrier concentration decreased with increment of Na doping from $3.2 \times 10^{16} \text{ cm}^{-3}$ to $2.5 \times 10^{13} \text{ cm}^{-3}$. The oxygen vacancies caused by the presence of Na ions compensates the electrons in the as-grown ZnO (which is n type in nature), thus leads to the decrease of carrier concentration with increase of Na ions. It is also worth to note that the carrier concentrations drop sharply to a very low level, however it still remains as n-type in character. Taking into consideration the highly insulating nature of ZnO, it seems to argue against the explanation of enhancement in magnetic ordering as a result of increased carrier concentration as shown by studies on bulk samples [39]. According to the widely used carrier-induced ferromagnetic mechanism [22,40], a large amount of free carriers and mobility are two important factors to get room temperature ferromagnetism. As recent studies reported, a ferromagnetic exchange mechanism which involves a spin-polarized electron trapped at an

oxygen vacancy [41]. An electron trapped in the oxygen vacancy constitutes an F-center (bound magnetic polaron), where the electron occupies an extended orbital state that overlaps with the d shells of several nearby transitional metal atoms, and this kind of direct ferromagnetic interaction was expected to be the main exchange mechanism.

In our ZnFeNaO system, Na ions enter into Zn sites forming p-type defects, and the room temperature ferromagnetism by Na co-doping can be explained in terms of a model of indirect exchange via Na related defects. Similar phenomenon has been found in the Na and Co co-doping ZnO samples [32]. These oxygen vacancies introduced by Na ions which coupled with electrons acted as F-centers, and it is helpful to the ferromagnetic coupling of Fe^{2+} . Our experimental results exhibit enhanced ferromagnetic couplings at room temperature in the sample of ZnFeO after Na co-doping, where the entry of Na^+ leads to an effective F-center mediation in ferromagnetic exchange interaction. The above results also show that magnetic states can be tuned by changing the defect concentration. Here with p-type Na dopants into the Fe-doped ZnO DMS lattice, the saturation magnetizations increase with the increment of Na ions. It can also be found that a very strong dependence of the magnetization on carrier density in $Zn_{0.95-x}Fe_{0.05}Na_xO$ ($x=0, 0.01, 0.05, 0.10$) samples, as depicted in Fig. 5. The magnetic moments increase in the Fe-doped ZnO DMS samples, which can be attributed to the increase of electron trapped oxygen vacancies. The increase of the magnetization with the increase of the Na concentration can also preclude the presence of Fe cluster or Fe related oxides for the magnetic ordering would not change significantly with increase of Na.

4. Conclusion

In summary, single-phase $Zn_{0.95-x}Fe_{0.05}Na_xO$ compound nanoparticles can be prepared by sol-gel method. Dopant Fe is in existence of Fe^{2+} in ZnO lattice. Structural characterizations revealed that Fe and Na ions enter into ZnO lattice without any secondary phase. The strong ferromagnetic behaviors at room temperature were found in all samples, and an enhanced ferromagnetic behavior was observed in $Zn_{0.95-x}Fe_{0.05}Na_xO$ nanoparticles, which can be attributed to the exchange interaction via electron trapped oxygen vacancies coupled with the magnetic Fe ions. With the increase of the Na ions, the oxygen vacancy mediated Fe^{2+} exchange ferromagnetic state become predominant, and therefore the magnetization shows a continuous increase. The results show clearly a correlation between the Na concentration, the carrier concentration and the ferromagnetic properties in the Na and Fe co-doped ZnO system.

Acknowledgment

This work is supported by National Natural Science Foundation of China (NSFC-50971113, 51171169 and 51102213).

References

- [1] J.K. Furdyna, *J. Appl. Phys.* 64 (1988) R29.
- [2] T. Dietl, H. Ohno, F. Matsukura, J. Cibert, D. Ferrand, *Science* 287 (2000) 1019.
- [3] S.A. Wolf, *Science* 294 (2001) 1488.
- [4] X. Zhou, S. Ge, D. Yao, Y. Zuo, Y. Xiao, *J. Alloys Compd.* 463 (2008) L9.
- [5] L.H. Van, M.H. Hong, J. Ding, *J. Alloys Compd.* 449 (2008) 207.
- [6] K. Sato, H. Katayama-Yoshida, *Semicond. Sci. Technol.* 17 (2002) 367.
- [7] P. Gopal, N.A. Spaldin, *Phys. Rev. B* 74 (2006) 094418.
- [8] H.J. Lee, S.Y. Jeong, C.R. Cho, C.H. Park, *Appl. Phys. Lett.* 81 (2002) 4020.
- [9] Y. Saeed, S. Nazir, H. Ali, A. Reshak, Shaukat, *J. Alloys Compd.* 508 (2010) 245.
- [10] Y.M. Kim, M. Yoon, I.-W. Park, Y.J. Park, J.H. Lyou, *Solid State Commun.* 129 (2004) 175.
- [11] R.K. Singhal, M. Arvind Samariya, Y.T. Xing, S. Kumar, S.N. Dolia, U.P. Deshpande, T. Shripathi, E.B. Saitovitch, *J. Alloys Compd.* 496 (2010) 324.

- [12] Y. Liu, J.H. Yang, Q.F. Guan, L.L. Yang, Y.J. Zhang, Y.X. Wang, B. Feng, J. Cao, X.Y. Liu, Y.T. Yang, M.B. Wei, *J. Alloys Compd.* 486 (2009) 835.
- [13] Q.Y. Xu, Z. Wen, L.G. Xu, J.L. Gao, D. Wu, K. Shen, T. Qiu, S.L. Tang, M.X. Xu, *Phys. B* 406 (2011) 19.
- [14] R.K. Singhal, P. Kumari, A. Samariya, S. Kumar, S.C. Sharma, Y.T. Xing, E.B. Saitovitch, *Appl. Phys. Lett.* 97 (2010) 172503.
- [15] R.K. Singhal, S. Kumar, P. Kumari, Y.T. Xing, E. Saitovitch, *Appl. Phys. Lett.* 98 (2011) 092510.
- [16] Z.L. Lu, W. Miao, W.Q. Zou, M.X. Xu, F.M. Zhang, *J. Alloys Compd.* 494 (2010) 392.
- [17] M.L. Dinesha, H.S. Jayanna, S. Mohanty, S. Ravi, *J. Alloys Compd.* 490 (2010) 618.
- [18] L.Q. Zhang, Z.Z. Ye, B. Lu, J.G. Lu, Y.Z. Zhang, L.P. Zhu, J.Y. Huang, W.G. Zhang, J. Huang, J. Zhang, J. Jiang, K.W. Wu, Z. Xie, *J. Alloys Compd.* 509 (2011) 2149.
- [19] Q.Y. Xu, S.Q. Zhou, H. Schmidt, *J. Alloys Compd.* 487 (2009) 665.
- [20] K. Sato, H. Katayama-Yoshida, *Jpn. J. Appl. Phys.* (2001) L334.
- [21] D.A. Schwartz, D.R. Gamelin, *Adv. Mater.* 16 (2004) 2115.
- [22] O.D. Jayakumar, I.K. Gopalakrishnan, K. Shashikala, S.K. Kulshreshtha, C. Sudakar, *Appl. Phys. Lett.* 89 (2006) 202507.
- [23] G.Y. Ahn, S.-I. Park, S.J. Kim, B.W. Lee, C.S. Kim, *IEEE Trans. Mag.* 41 (2005) 2730.
- [24] M.H.F. Sluiter, Y. Kawazoe, P. Sharma, A. Inoue, A.R. Raju, C. Rout, U.V. Waghmare, *Phys. Rev. Lett.* 94 (2005) 187204.
- [25] P. Mills, J.L. Sullivan, *J. Phys. D: Appl. Phys.* 16 (1983) 723.
- [26] J.N. Zhou, A. Butera, H. Jiang, D.H. Yang, J.A. Barnard, *J. Appl. Phys.* 85 (1999) 6151.
- [27] J.T. Luo, Y.C. Yang, X.Y. Zhu, G. Chen, F. Zeng, F. Pan, *Phys. Rev. B* 82 (2010) 014116.
- [28] S. Kumar, Y.J. Kim, B.H. Koo, S.K. Sharma, J.M. Vargas, M. Knobel, S. Gautam, K.H. Chae, D.K. Kim, Y.K. Kim, C.G. Lee, *J. Appl. Phys.* 105 (2009) 07C520.
- [29] G.Y. Ahn, S.-I. Park, C.S. Kim, *J. Magn. Magn. Mater.* 303 (2006) e329.
- [30] J.A. Raley, Y.K. Yeo, R.L. Hengehold, M.Y. Ryub, T.D. Steiner, *J. Alloys Compd.* 423 (2006) 184.
- [31] O.D. Jayakumar, I.K. Gopalakrishnana, R.M. Kadamb, A. Vinuc, A. Asthanad, K.V. Rao, A.K. Tyagia, *J. Cryst. Growth* 307 (2007) 315.
- [32] H. Gu, Y.Z. Jiang, Y.B. Xu, M. Yan, *Appl. Phys. Lett.* 98 (2011) 012502.
- [33] E.-C. Lee, K.J. Chang, *Phys. Rev. B* 70 (2004) 115210.
- [34] S.B. Orlinskii, J. Schmidt, P.G. Baranov, D.M. Hofmann, C.M. Donega, A. Meijerink, *Phys. Rev. Lett.* 92 (2004) 047603.
- [35] D.Y. Wang, S.X. Gao, *J. Alloys Compd.* 476 (2009) 925.
- [36] M.G. Wardle, J.P. Goss, P.R. Briddon, *Phys. Rev. B* 71 (2005) 155205.
- [37] R.K. Singhal, A. Samariya, S. Kumar, Y.T. Xing, U.P. Deshpande, T. Shripathi, E.B. Saitovitch, *J. Magn. Magn. Mater.* 322 (2010) 2187.
- [38] A.G. Joshi, S. Sahai, N. Gandhi, Y.G. Radha Krishna, D. Haranath, *Appl. Phys. Lett.* 96 (2010) 123102.
- [39] O.D. Jayakumar, I.K. Gopalakrishnana, S.K. Kulshreshtha, *J. Mater. Chem.* 15 (2005) 3514.
- [40] T. Zhao, S.R. Shinde, S.B. Ogale, H. Zheng, T. Venkatesan, R. Ramesh, S. Das Sarma, *Phys. Rev. Lett.* 94 (2005) 126601.
- [41] J.M.D. Coey, A. Douvalis, C. Fitzgerald, M. Venkatesan, *Appl. Phys. Lett.* 84 (2004) 1332.